Article

Experimental Investigation of Dimensional Precision of Deep Drawn Cups Using Direct Polymer Additive Tooling

Georg Bergweiler, Falko Fiedler [ID]**, Ahsan Shaukat and Bernd Löffler** *

Laboratory for Machine Tools and Production Engineering (WZL), RWTH Aachen University,
52074 Aachen, Germany; g.bergweiler@wzl.rwth-aachen.de (G.B.); f.fiedler@wzl.rwth-aachen.de (F.F.);
ahsan.shaukat@wzl.rwth-aachen.de (A.S.)
* Correspondence: b.loeffler@wzl.rwth-aachen.de; Tel.: +49-175-642-520-8

Abstract: While deep drawing of sheet metals is economical at high volumes, it can be very costly for manufacturing prototypes, mainly due to high tooling costs. Additively manufactured polymer tools have the potential to be more cost-efficient for small series, but they are softer and thus less resilient than conventional steel tools. This work aimed to study the dimensional precision of such tools using a standard cup geometry. Tools were printed with FFF using two different materials, PLA and CF-PA. A test series of 20 parts was drawn from each tool. Afterwards, the dimensional precisions of the drawn parts were analyzed using an optical measuring system. The achieved dimensional accuracy of the first drawn cup using the PLA toolset was 1.98 mm, which was further improved to 1.04 mm by altering shrinkage and springback allowances. The repeatability of the deep drawing process for the CF-reinforced PA tool was 0.17 mm during 20 drawing operations and better than that of the PLA tool (1.17 mm). To conclude, deep drawing of standard cups is doable using direct polymer additive tooling with a dimensional accuracy of 1.04 mm, which can be further improved by refining allowances incorporated to the CAD model being printed.

Keywords: deep drawing; fused filament fabrication; rapid prototyping; rapid tooling; 3D-printing; car body manufacturing; forming tool

1. Introduction

Many industrial sectors are under pressure to reduce development costs and time to market. Global trends such as individualization, increased numbers of derivatives, and shorter product life cycles are enhancing the pressure to innovate. Sheet metal forming is a production process, which is especially affected by these trends due to a high level of automation and high up-front investments for tools. Therefore, sheet metal drawn parts are usually only economical in large-scale production. To produce prototypes, cheaper tools such as milled polymers or casted resins are used to reduce cost [1–3]. These tools are manufactured in multiple steps, which often include manual work [1]. This is one aspect that still makes the process cost-intensive and time-consuming. Direct polymer additive tooling (DPAT) is an alternative tooling method, which aims to further reduce production costs and time for small-lot production. In contrast to indirect tooling methods, the tools are directly manufactured using polymer additive manufacturing (AM) technologies. While DPAT is a widely researched topic for manufacturing injection molds [4–6], it has been almost entirely neglected for the production of deep drawing tools. Most studies addressing the applications of DPAT in the field of sheet metal forming are dealing with bending or embossing operations. Deep drawing, as one of the most common forming processes, has not been systematically studied yet.

Manufacturing of a sheet bending tool using additive manufacturing methods, such as fused filament fabrication (FFF) and selective laser sintering (SLS), was already patented in 2013 [7]. Another study proposed using laser beam melting to create tools for the hot forming sheet metal process of press hardening [8]. These studies focused on specialized

parts with pre-defined unique geometries and did not cover the feasibility of additive manufacturing for the process in general. Secondly, these processes mainly include manufacturing a metal die using additive manufacturing, which can reduce production times but requires expensive equipment (laser sintering printers, sheet lamination printers). Low cost, desktop, or small workshop ready additive manufacturing alternatives have not been presented in these investigations.

The research by Durgun is focused more on low-cost polymer printing using desktop fused deposition modeling (FDM) technology to create dies for sheet metal forming [9]. In that research, a tailgate lock reinforcement bracket was manufactured using FDM of polymer material. A study by Aksenov investigated the manufacturing of micro heat exchangers by using FDM printed tools to bend thin aluminum sheets [10]. Multiple v-bend dies of varying width and heights were printed and used. Another study to investigate the v-bend forming using printed tools was done by Nakamura [11]. Schuh investigated the use of FDM-tools by carrying out the cupping test according to Erichsen, and further improved the stiffness of such tools by adding screw elements [12]. Cheah and Du analyzed sheet metal embossing using 3D-printed polymer tools, whereas Leacock studied the application of DPAT for the stretch forming process of aluminum sheets [13–15]. These studies not only showed the basic feasibility of the tools but also pointed out advantages regarding production cost and time. All studies have in common that specific use cases were studied, which makes it difficult to transfer the results to other tool and part geometries. Additionally, the mentioned publications analyzed forming processes, such as bending or embossing, which usually experience lower degrees of deformation than deep drawing.

This work aimed to study the behavior of deep drawing tools, manufactured with DPAT, using a standard cup geometry. Two different FFF materials, PLA and CF-reinforced PA, were used for the experiments. The tool wear and the dimensional precisions of the cups were determined as indicators to show the feasibility of this tooling technique in general.

2. Methodology

2.1. Deep Drawing

In this process, a flat sheet is formed into various shapes like boxes, cylinders, and cones by using a punch that draws the metal to flow between a die and a blank holder. The basic components of most deep drawing operation toolsets are punch, blank holder, and die. Figure 1 shows the basic principle of the deep drawing process of a cup shape. The sheet metal blank (I) is held between the blank holder (II) and the die (III) and is pressed with the punch (IV), forming the blank into the desired shape.
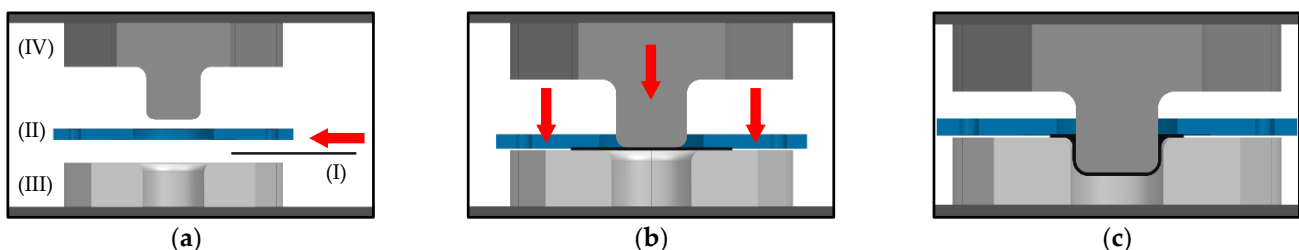

Figure 1. Working principle of deep drawing: (**a**) a sheet metal blank is inserted between die and blank holder; (**b**) forces on both the blank holder and the punch are applied; (**c**) final cup geometry including a flange is formed.

2.2. Fused Filament Fabrication

Fused Filament Fabrication (FFF) or Fused Deposition Modelling (FDM) is a widely used and commonly available AM process on the market. In this process, a polymer material (usually in the form of filament or granules) is molten to a semi-solid state using

heat and forced through a nozzle. Figure 2 shows the basic working principle of the FFF process. The nozzle (I) moves to trace out the desired cross-section from the CAD model on the built platform (II). With the aid of a support structure (III), usually built with a second material that can be removed, overhangs can be printed. The bed moves one layer in height and the next layer is started.
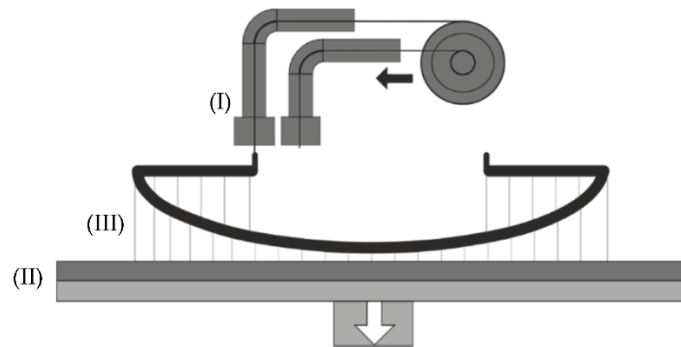

Figure 2. Working principle of FFF process [16] (reproduced with the permission of the Verein Deutscher Ingenieure e.V.).

A variety of pure polymer and reinforced materials are available on the market. Reinforcement is done by adding microfibers to the filament during filament production. These fibers increase certain mechanical properties, which usually comes at a cost of flexibility. Compressive strength and cost are considered as the main criteria relevant to this application. Since compressive strength data of most filament materials are not available, an assumption is made that materials having high tensile and flexural strengths tend to have high compressive strength. Figure 3 gives an overview of mechanical properties of commonly available FFF materials including their cost.
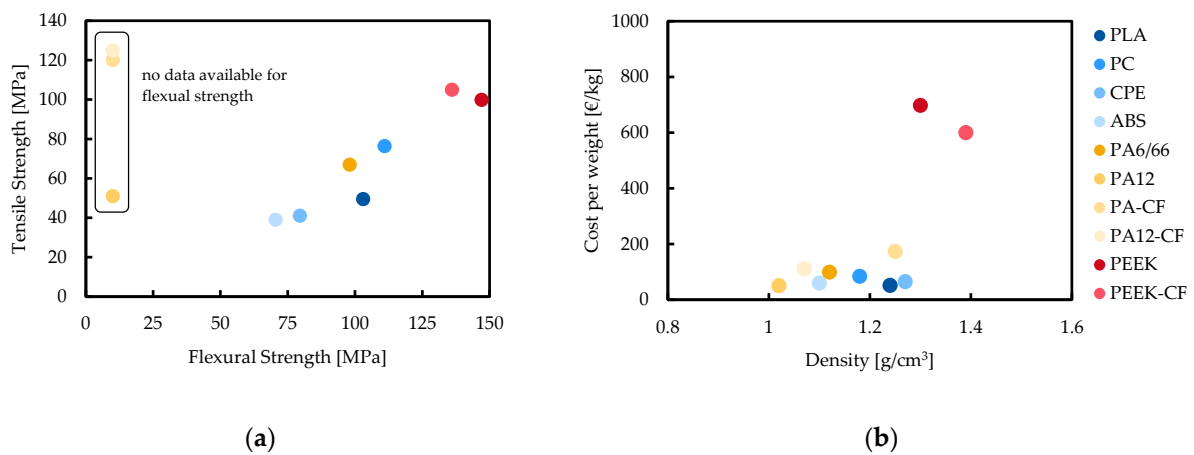

(**a**) (**b**)

Figure 3. Properties of different AM polymers (for abbreviations and chemical formulae, see Appendix A): (**a**) tensile strength plotted over flexural strength; (**b**) cost per kilogram plotted over density [17–26].

The selected materials based on these criteria are PLA and CF-reinforced PA. Despite being a low cost material, PLA still shows decent mechanical properties. CF-PA is chosen as one of the high-performance material, since the cost is much less than that of PEEK material. The mechanical properties of these materials are summarized in Table 1.

Table 1. Material properties of PLA and CF-reinforced PA [17,18].

Property	Test Method	Unit	PLA	CF-PA
Yield strength	ISO 527	MPa	49.5	120.0
Tensile modulus	ISO 527	MPa	2346.5	14,400.0
Elongation at break	ISO 527	%	5.20	0.98
Compressive strength	ISO 527	MPa	no data	112.73
Flexural strength	ISO 178 (PLA)	MPa	103	no data
Flexural modulus	ISO 178 (PLA) ISO 14125 (CF-PA)	MPa	3150	4780
Density	ASTM D1505 (PLA) ISO 1183 (CF-PA)	g/cm^3	1.24	1.25

2.3. Workpiece Specifications and Tool Design

The blank material used for the experiments is DC04 with a thickness of 1 mm, which is a cold rolled steel according to DIN EN 10130, commonly used for deep drawing [27]. The mechanical properties are summarized in Table 2.

Table 2. Mechanical properties of DC04 [27].

Material	Yield Strength	Ultimate Strength	Elongation at Break
DC04	210 MPa	270–350 MPa	38%

The design of the workpiece geometry is done in such a way that the tools experience significant stress that typically occurs in a deep drawing process. This is done by setting the drawing ratio at β = 2.2, which is slightly higher than the limiting drawing ratio for DC04 (β_0 = 2.125). The limiting drawing ratio indicates the maximum ratio of a circular blank diameter to the die diameter, without crack formation [28]. In addition to a high drawing ratio, the punch nose and die corner radii are set to a small value according to *Dietrich* and *Fritz*, which further increases stress [29,30]. The drawing depth is set to 14 mm so that a flange of around 8 mm is formed. Clearance C is the space between the punch and die and is slightly higher than the blank thickness for smooth operation. It can be calculated according to *Dietrich* [29]. The used specifications of the workpiece are illustrated in Figure 4 and summarized in Table 3.
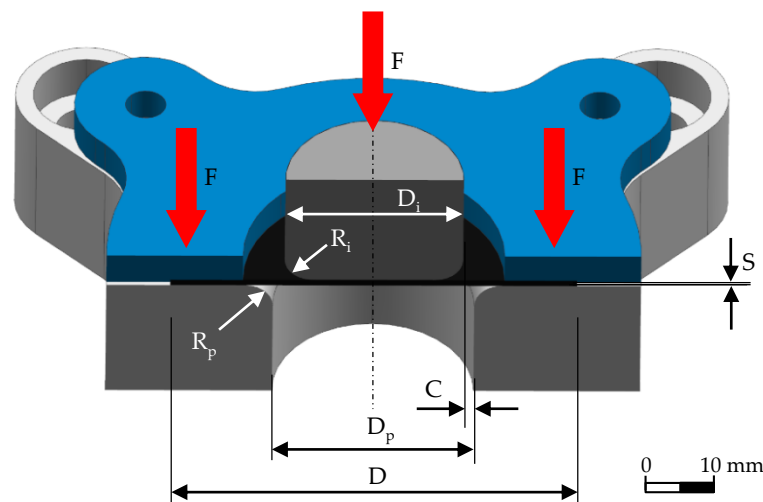

Figure 4. Schematic of deep drawing parameters.

Table 3. Deep drawing specifications.

No.	Feature	Symbol	Value (mm)
1	Inside cup diameter	d_o	25
2	Blank diameter	D	55
3	Drawing ratio	β	2.2 (no unit)
4	Blank thickness	S_o	1
5	Drawing depth	h_o	14
6	Clearance	C	1.34
7	Die diameter	D_p	27.68
8	Punch diameter	D_i	25
13	Die corner radius	R_p	5
14	Punch nose radius	R_i	3.75

Each tool is designed to reduce the use of material to be printed and to make it compatible for the mounting on the pillar die set. For all experiments, the blank holder design is kept the same. It is a thin part with 100% infill and does not experience any noticeable shrinkage to be compensated. An isometric view of the punch, die and the blank holder is shown in Figure 5.
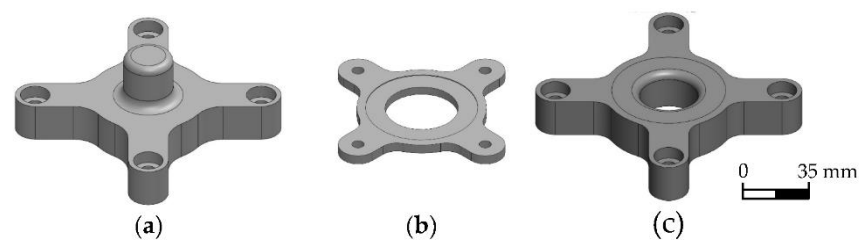

(a)   (b)   (c)

Figure 5. Isometric view of the tools including mounting holes: (**a**) punch; (**b**) blank holder; (**c**) die.

2.4. Printing Specifications

Printing parameters differ from material to material. For a standardized comparison, parameters relating to the amount and position of material in the printed part are kept the same. These parameters include layer height, infill pattern and ratio, wall thickness, and shell thickness. The values of these parameters are selected in a way that lies in the recommended setting by the manufacturer for all these materials [17,31]. In the first trial of experiments PLA and CF-PA are investigated, while in the second trial of experiments the tool geometry is adjusted for PLA: Table 4 gives an overview of the printing parameters to be used.

Table 4. Printing parameters of PLA, 1st and 2nd trial and CF-reinforced PA.

No.	Property	PLA 1st Trial	CF-PA	PLA 2nd Trial
1	Layer height (mm)	0.2	0.2	0.2
2	Shell thickness (mm)	2.4	2.4	2.4
3	Infill type	Triangles	Triangles	Triangles
4	Infill percentage (%)	80	80	80
5	Nozzle temperature (°C)	200	280	200
6	Build plate temperature (°C)	60	80	60
7	Print speed (mm/s)	70	50	70
8	Fan cooling	Yes	No	Yes
9	Support	No	No	No
10	Build plate adhesion	Brim	Brim	Brim

An Ultimaker S5 printer is used that works by Fused Filament Fabrication (FFF). It has a dual nozzle with a maximum print volume of $330 \times 240 \times 300$ in X-, Y-, and Z-axis, respectively. The filament used is 2.85 mm in diameter and the nozzle diameter, which

determines the layer resolution, is 0.4 mm. The specified print resolution (precision of printing) is 6.9 μm in the X-Y-plane and 2.5 μm on Z-axis. The maximum achievable nozzle and bed temperatures are 280 °C and 140 °C, which fulfill all the printing requirements for these experiments.

As a result of the layer-by-layer buildup of the FFF process, every radius, which is shaped by different layers show a so called stair stepping effect. This effect can be seen in Figure 6 of a probe with a 3 mm radius printed with CF-PA and the printing parameters as mentioned above. The surface finish of PLA is smooth compared to CF-PA. Both the stair stepping effect and the surface roughness of the tools will affect the precision of the drawing process. Considering the comparably low hardness of the materials, the surface roughness will be smoothened during the forming process, leaving no scratches on the formed parts. Except from removing the brim of the printed tools no post-processing was carried out on the tools.
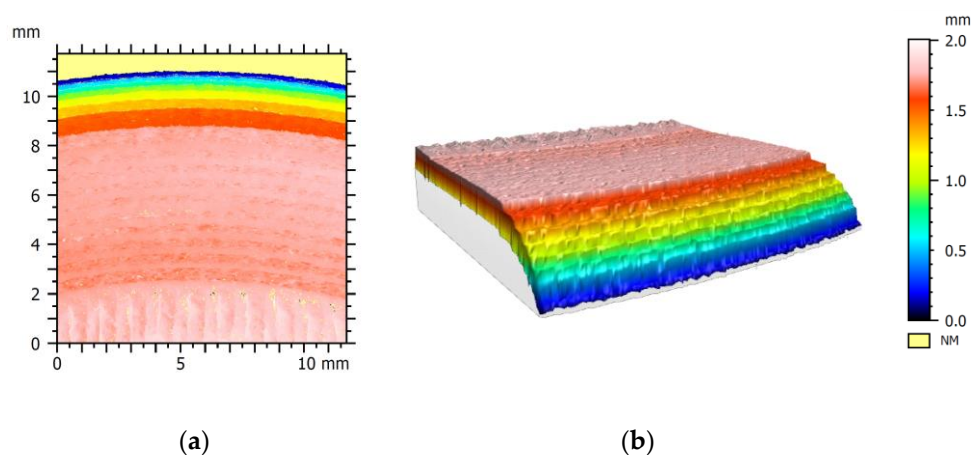

(**a**) (**b**)

Figure 6. Surface scans of CF-PA material showing the stair stepping effect at a radius of 3 mm: (**a**) vertical view; (**b**) isometric view.

2.5. Experimental Setup

The experiments are carried out using a Lindenberg TP-20 2702 hydraulic press with a Siemens Two-Hand operation console, sourced from Lindenberg Technics AG in Altendorf, Switzerland. The press has a loading capacity of 196.2 kN and a maximum travel distance (without any toolset) of 250 mm. The scanning and recording of measurements are performed by Nikon MCAx35+ arm with ModelMaker H120, sourced from Nikon Metrology GmbH in Alzenau, Germany. The system has an accuracy of 0.048 mm, while its measuring range is 3.5 m. The measurements are recorded using the software PolyWorks Inspector, sourced from Duwe-3d AG in Lindau, Germany. Afterward, the data are exported in the form of polygon models and compared with the reference CAD geometries in GOM Inspect Professional software, sourced from GOM GmbH in Brunswick, Germany.

2.6. Experimental Procedure

The experiments are carried out in two stages: In the first trial of experiments PLA and CF-PA tools are printed considering general shrinkage recommendations. To further improve the dimensional accuracy of the tools, a second trial of experiments with PLA material was carried out to study the effect of adding allowances. In the first trial, 20 cups are drawn from each tool material and optically scanned. Scanning of the printed tools is done before any drawing operation (zeroth draw) and then after every five drawing operations to minimize scanning effort.

The second trial of experiments is conducted after incorporating additional shrinkage corrections in the CAD model for the PLA tools, thus starting with a slightly different tool

geometry. The scanning for each cup is performed as before but the polymer tools are scanned after every two drawing operations in order to get more data points.

　　　　To measure and compare the deviation results, a set of measuring points are defined on the tool and part geometries and standardized throughout all scans. For improved accuracy, an average of eight points spread evenly across the entire periphery is taken for each set of measurements (cf. Figure 7b). The selected measuring points on the cup, punch, and die are shown in Figure 7 and the evenly distributed eight points exemplary on the cup surface.
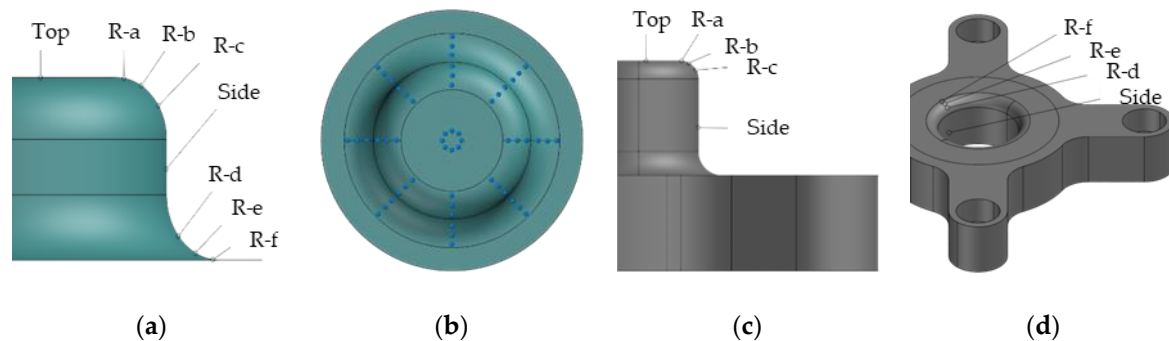

(a)　　　　　　　　　　(b)　　　　　　　　　　(c)　　　　　　　　　　(d)

Figure 7. Measuring points of tool and cup surface: (**a**) measuring points distribution for cup; (**b**) distribution of eight sets of points for average (here exemplary on cup surface); (**c**) measuring points distribution for punch; (**d**) measuring points distribution for die.

　　　　　　The scanned cups and tools are compared with the reference CAD model to check the absolute value of deviations on the defined points for both cups and tools. This comparison is performed for each material in the beginning and at the end of the test series. First, the deviations of printed tools before any drawing operation (zeroth draw) are noted and compared with the deviations of first drawn cups. Then the deviations of printed tools on the second to last scan, that is after the 15th drawing operation are compared with the 20th drawn cups deviations. The reason for taking the 15th drawn tool's deviations is because the scanning interval of tools for PLA's first trial and CF-PA is after every 5 draws. This frequency was further refined in the second trial of PLA where the tools were scanned after every two draws. The first comparison shows the dimensional accuracy before any drawing operation and the second comparison shows the dimensional accuracy after 20 drawing operations. For PLA's first trial with allowances incorporated, the 18th drawn tool's scans are used with 20th drawn cups to perform the second comparison.

　　　　　　Colored 3D mapped deviation graphs are used to visualize differences in deviations from the reference geometry. Deviation values from the predefined points are compared in a bar chart to understand the behavior of these changes. Figure 8 shows a color map for the comparison of a scanned outer surface of a cup and its underlying reference geometry. The green color indicates no deviation (with a tolerance of ±0.05 mm). Positive deviations (more material) are those, which cross the reference surface on the outside and are shown as colors changing from yellow to brown as the deviation intensity increases. Negative deviations (less material) are those which cross the reference surface on the inside and are shown as colors changing from light blue to purple with increasing deviation. For an easier understanding of the visual color maps of deviations and the bar charts, the direction of deviations (positive or negative) in each part is adjusted to align with the deviation direction of the outer scan of the cups.
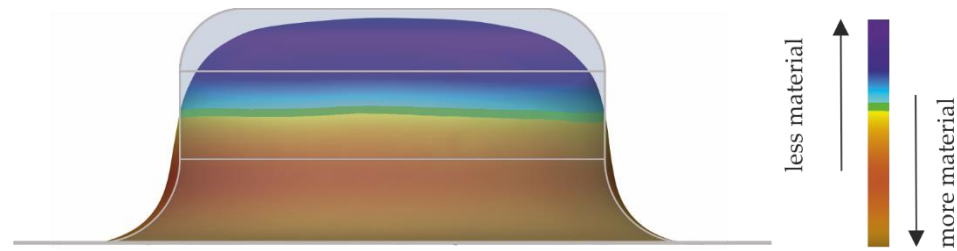
Figure 8. Scanned outer surface of a cup compared to its reference geometry (the comparison to the CAD geometry is exaggerated for easier understanding).

3. Results

3.1. Dimensional Accuracy and Precision of Deep Drawn Cups—First Trial

The deviation values of the eight predefined measuring points of the zeroth drawn tool and first drawn cup for PLA and CF-reinforced PA are compared in a pillar chart in Figures 9a and 10a respectively. The deviation of tools, which are noted before any drawing operation is a result of the accuracy of printing. A graphical color map depiction of the cup deviations is shown in the second column (b) of Figures 9 and 10. The third column (c) shows the color map of the 20th drawn cup compared to the CAD reference geometry, followed by the pillar chart for 15th drawn tool and 20th drawn cup.
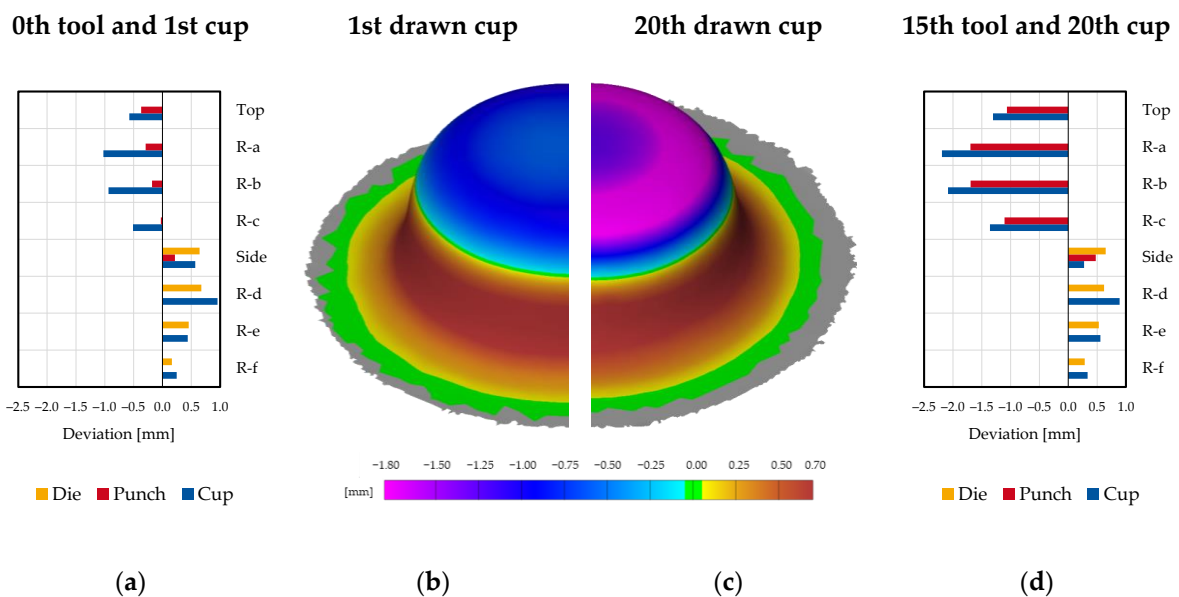

Figure 9. Deviation values of PLA tools and their drawn cups compared to their CAD reference geometries: (**a**) pillar chart of the zeroth drawn tool and first drawn cup; (**b**) color map of the outer surface of first drawn cup; (**c**) color map of the outer surface of the 20th drawn cup; (**d**) pillar chart of the 15th drawn tool and 20th drawn cup.

The dimensional repeatability and precision of the drawn cups can be taken from Figures 11 and 12. As opposed to Figures 9 and 10, where the cups are compared to their CAD reference geometries, the colored map in Figure 11 shows the comparison of the 20th drawn cup of both PLA and CF-reinforced PA to the first drawn cup, which is taken as reference geometry. Figure 12 shows the deviation trend of 20 drawing operations of cups drawn from both materials. It can be observed that the deviations in points R-a, R-b, R-c, and top of PLA increase more during the 20 drawing operations compared to other points, indicating higher forces on the punch nose radius and the top. After the first draw, CF-reinforced PA and PLA cups show similar maximum deviations of −0.92 to 0.77 mm

and −1.02 to 0.96 mm, respectively. After 20 drawing operations, the deviations of cups drawn with PLA increase to −2.19 mm at the punch nose radius R-a. For CF-PA tools, only a minor increase on the radius R-a to −1.04 mm is stated. This behavior can be seen in Figure 11, where the cups drawn from CF-PA show much less change in deviation than those drawn from PLA. This shows that CF-reinforced PA resists deformation much better than PLA.
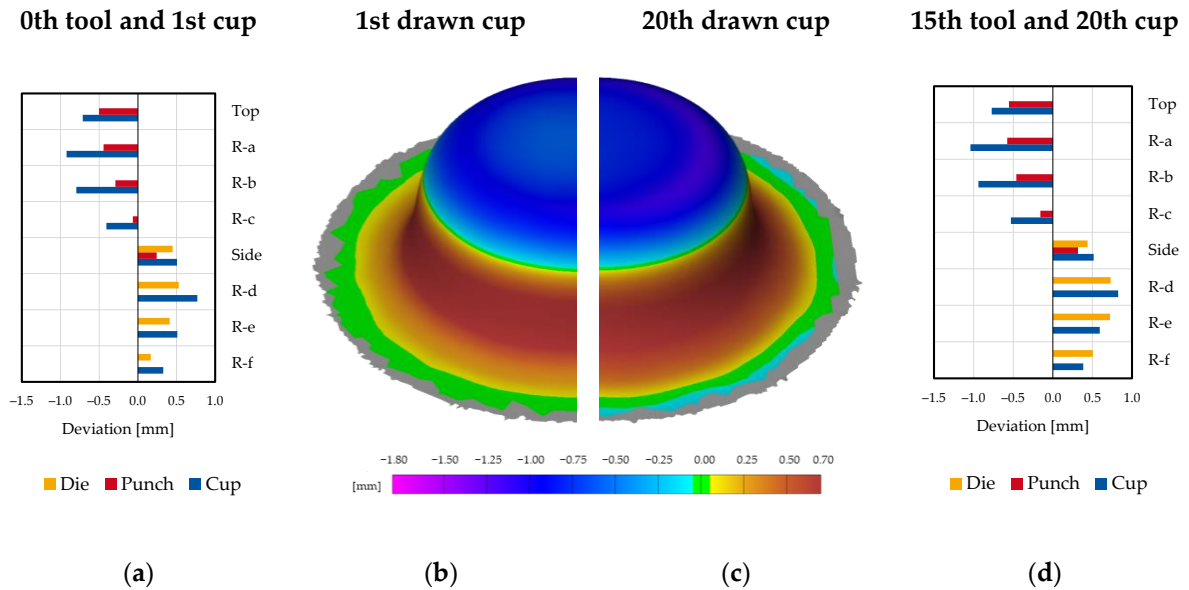
CF-reinforced PA

Figure 10. Deviation values of CF-reinforced PA tools and their drawn cups compared to their CAD reference geometries (please note the different scale of the pillar chart compared to Figure 9): (**a**) pillar chart of zeroth drawn tool and first drawn cup; (**b**) color map of the outer surface of the first drawn cup; (**c**) color map of the outer surface of the 20th drawn cup; (**d**) pillar chart of the 15th drawn tool and 20th drawn cup.
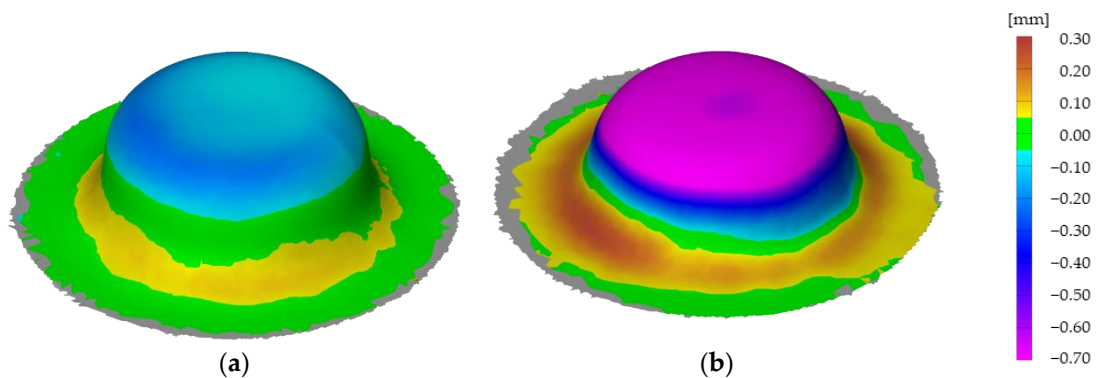

Figure 11. Color map of the outer surface of 20th drawn cup compared to the first drawn cup: (**a**) color map of cup drawn from CF-reinforced PA tools; (**b**) color map of cup drawn from PLA tools.

Figure 13 shows the deformations of the punch for both materials after 20 drawing operations compared to the first scan of punch. The color map can be interpreted as wear on the punch, which is equal to the plastic deformation of the tool. The die shows a similar behavior as the punch, but having less deformation over the 20 drawing operations, whereas the wear on the blank holder can be neglected. The growth of deviations for the CF-reinforced PA punch, shown in Figure 14a, is almost flat, whereas the deviations change more for the PLA punch, shown in Figure 14b. PLA shows higher growth of deviations

in the beginning, which tend to flatten after 5 to 10 drawing operations before starting to increase again after 15 drawing operations. With respect to the PLA punch, it can be seen that the longitudinal compression results, at least partially, in a lateral expansion of the material (cf. Figure 14b side and top). To conclude, CF-reinforced PA resists deformations much better than PLA.
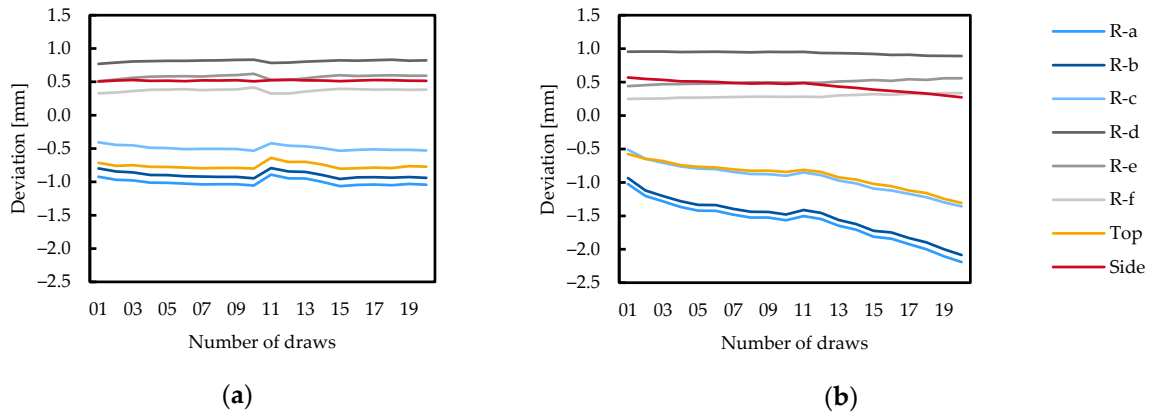

(a)

(b)

Figure 12. Deviation values of different measuring points of cups during 20 drawing operations compared to the CAD reference geometry: (**a**) deviation values of cups drawn from CF-reinforced PA tools; (**b**) deviation values of cups drawn from PLA tools.
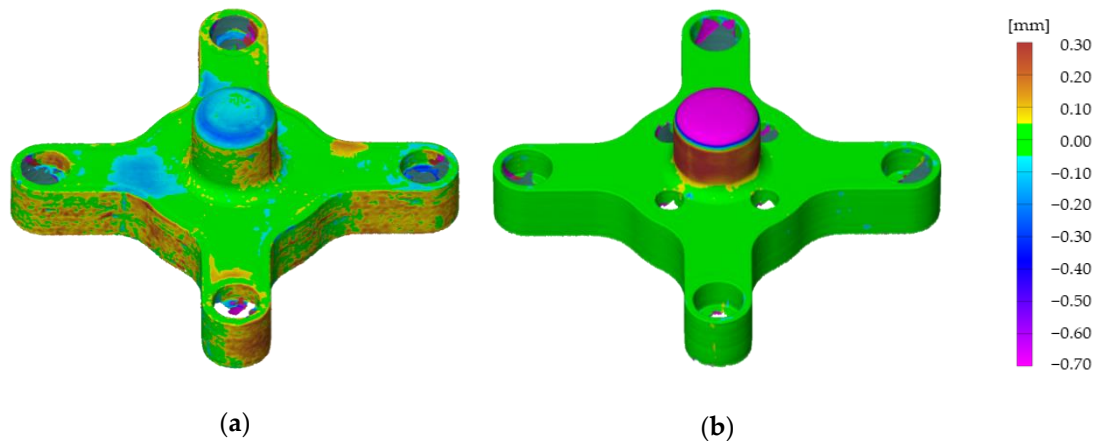

(a)

(b)

Figure 13. Color map of deviations of the 20th drawn punch compared to the zeroth drawn punch: (**a**) CF-PA punch; (**b**) PLA punch.
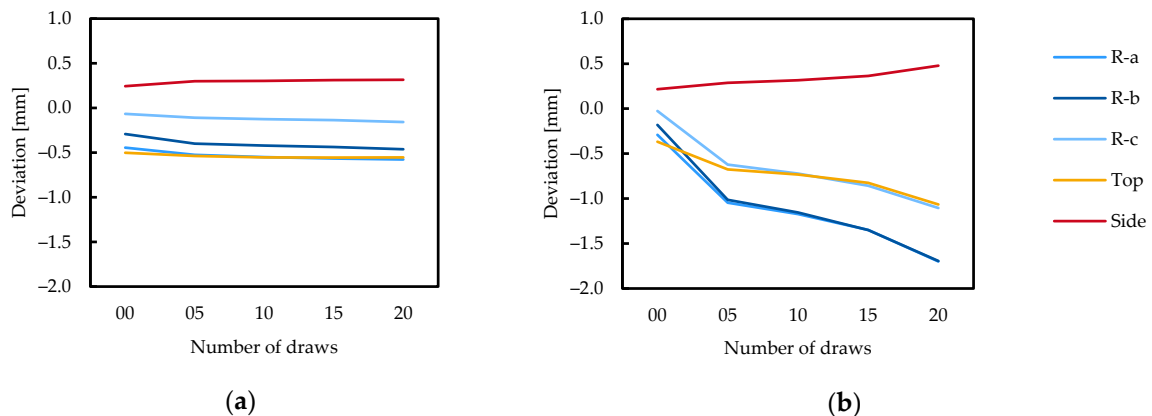

(a)

(b)

Figure 14. Course of deviation values of different measuring points of the punch during 20 drawing operations compared to the CAD reference geometry: (**a**) deviation values of CF-reinforced PA punch; (**b**) deviation values of PLA punch.

3.2. Effect of Adding Allowances on Dimensional Accuracy and Precision—Second Trial

When it comes to the dimensional accuracy or the absolute deviations of the drawn cups, the initial deviation values of the printed tools play a significant role. If the actual dimensions of the tools differ from their CAD geometries, that will also affect the cup's geometry (cf. pillar chart of Figures 9 and 10). This section deals with the effect of adding allowances to the dimensional accuracy and precision of the cups. Since the punch primarily experiences compression load, and thus compresses during the drawing operation, it was printed with excess material to compensate for the plastic deformation (cf. pillar chart of Figure 15c). The measurement data of PLA's first trial was used (from Section 3.1). After adding allowances in the second trial of PLA tools, cups were drawn and measured according to Section 2.6. The dimensional accuracies of cups drawn after 20 trials from PLA without allowances, from here onwards called PLA_001, and PLA with allowances, called PLA_002, are shown in Figure 15. Better accuracy was achieved even after 20 drawing operations by adding allowances to the printed parts.
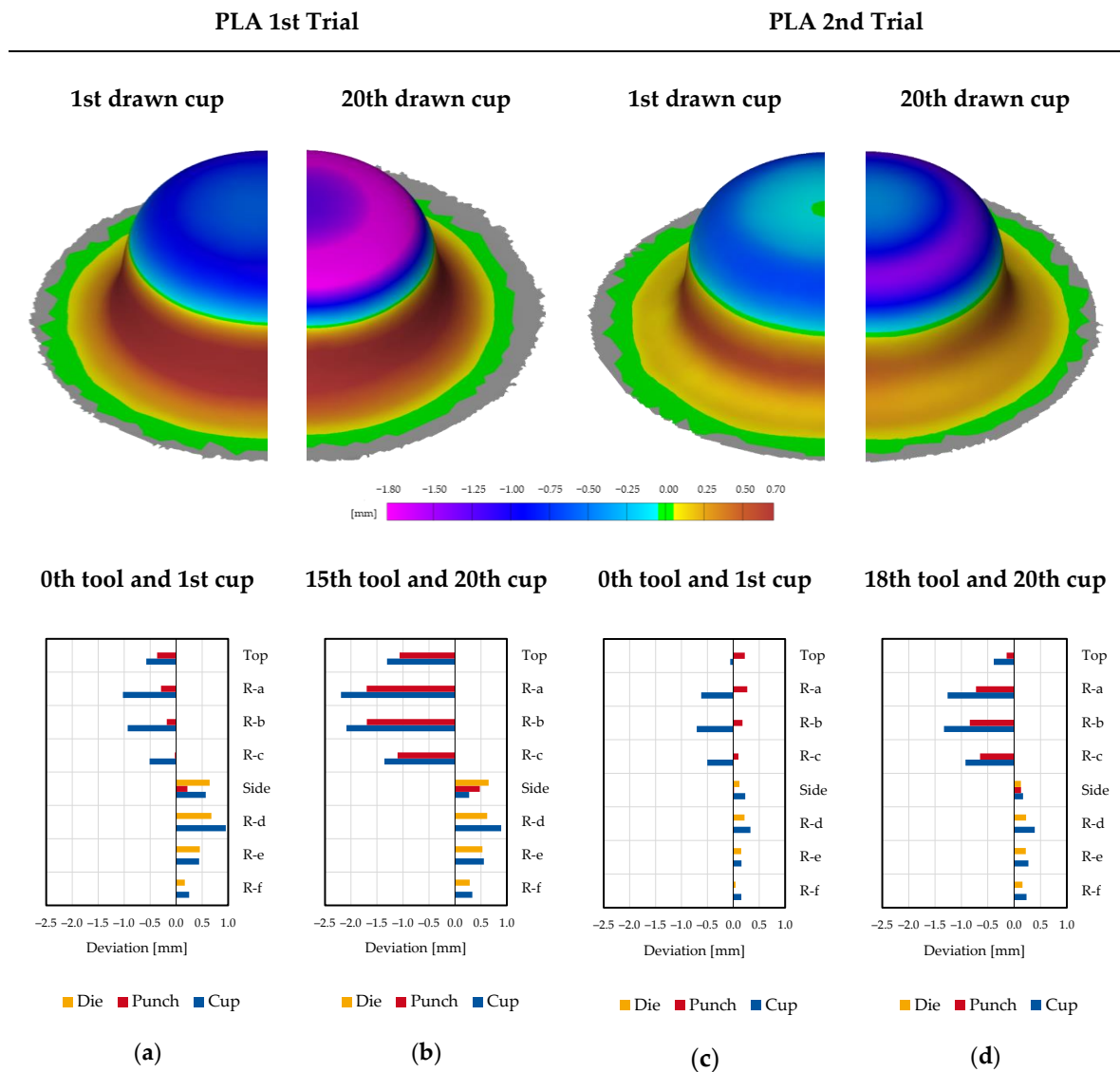

Figure 15. Deviation values of both trials of PLA tools and their drawn cups compared to their CAD reference geometries (please note the different scale of the pillar chart compared to Figure 10): (**a**) pillar chart of PLA_001 zeroth drawn tool and first drawn cup and color map of first drawn cup; (**b**) pillar chart of PLA_001 15th drawn tool and 20th drawn cup and color map of 20th drawn cup; (**c**) pillar chart of the PLA_002 zeroth drawn tool and first drawn cup and color map of first drawn cup; (**d**) pillar chart of the PLA_002 18th drawn tool and 20th drawn cup and color map of the 20th drawn cup.

As opposed to Figure 15, where the cups are compared to their CAD reference geometries, Figure 16 shows the color map of 20th drawn cup compared to the first drawn cup. After 20 drawing operations, the deviation of the cup drawn from PLA_002 was smaller than that of PLA_001. The highest deviations are noted at R-a, R-b, and R-c, which are points on the punch nose radius as shown in Figure 17. As mentioned in Section 3.1, the deviations of the first cup drawn from PLA_001 range from −1.02 to 0.96 mm. With allowances incorporated, the deviations of the first cup drawn from PLA_002 could be improved to a range from −0.71 to 0.33 mm. Over the course of 20 drawing operations, the deviations for PLA_002 cups increased to −1.33 and 0.39 mm, which are less than the deviations of PLA_001 cups, ranging from −2.19 to 0.89 mm. To conclude, having additional allowances incorporated in PLA's first trial not only decreases the deviation for the first cup, but also leads to a lesser increase of deviation over the course of 20 drawing operations.
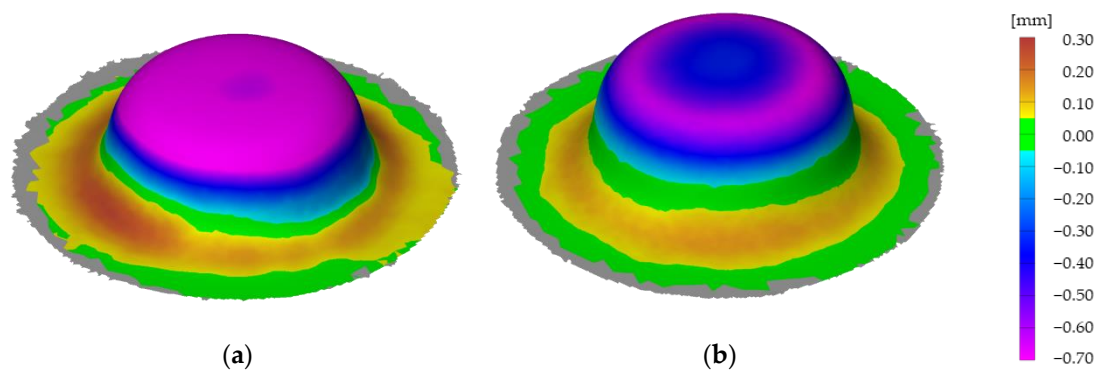

(**a**) (**b**)

Figure 16. Color map of deviations of 20th drawn cup compared to the first drawn cup for both PLA trials: (**a**) cup drawn with PLA_001 tool; (**b**) cup drawn with PLA_002 with allowances incorporated.
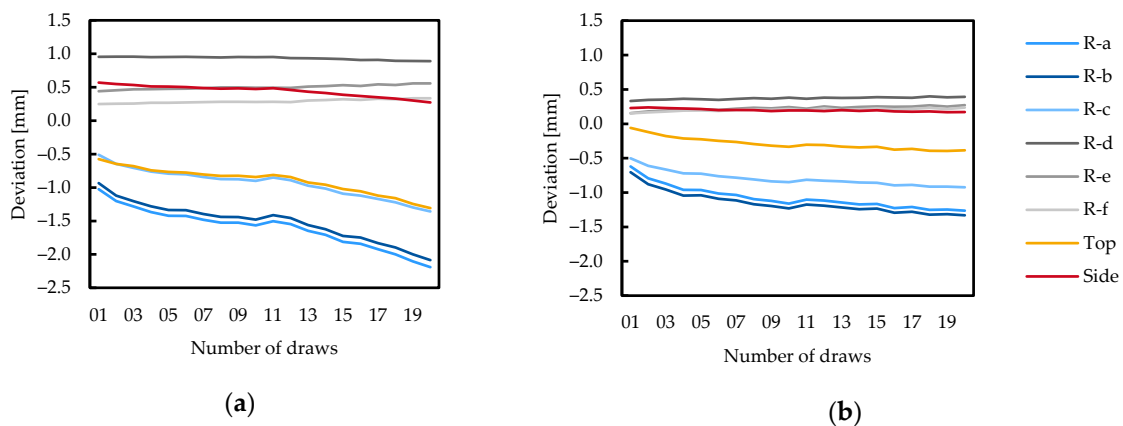

(**a**) (**b**)

Figure 17. Course of deviation values of different measuring points of the cup during 20 drawing operations compared to the CAD reference geometry: (**a**) deviation values of cups drawn with PLA_001 tool; (**b**) deviation values of cup drawn with PLA_002 tool.

The effect of adding allowances throughout 20 drawing operations in terms of deviations and wear on the PLA tool (punch) is shown in Figure 18. By adding allowances, the initial draw deformations in the plastic tool (punch) are reduced, and hence the accuracy is improved throughout 20 drawing operations. Figure 19 shows the course of deviation of the punch of both PLA trials. The span of deviation before any drawing operation (zeroth draw), is much higher for PLA_001 than of PLA_002. It can also be noticed that PLA_002 was printed with excess material (positive values of all measuring points at zeroth draw). This is beneficial over the course of the drawing operation, since all measuring points except the "side" compressed during the test series.
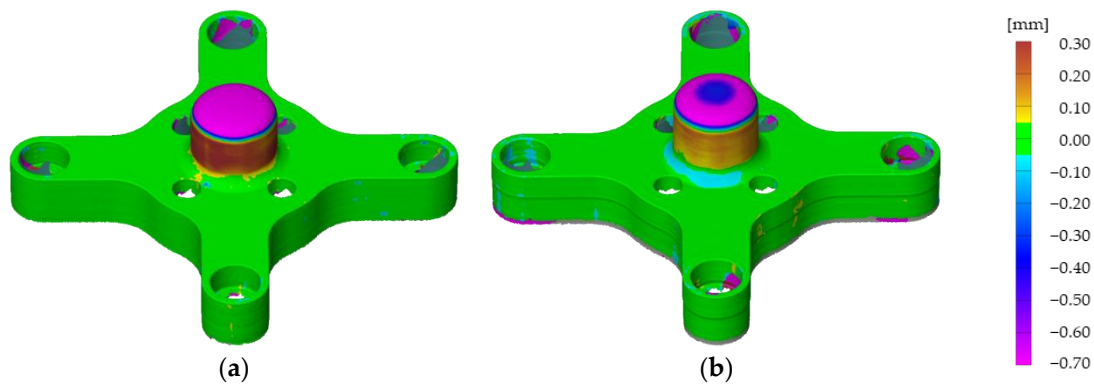
Figure 18. Color map of deviations of the 20th drawn punch compared to the zeroth drawn punch: (**a**) PLA_001 punch; (**b**) PLA_002 punch.
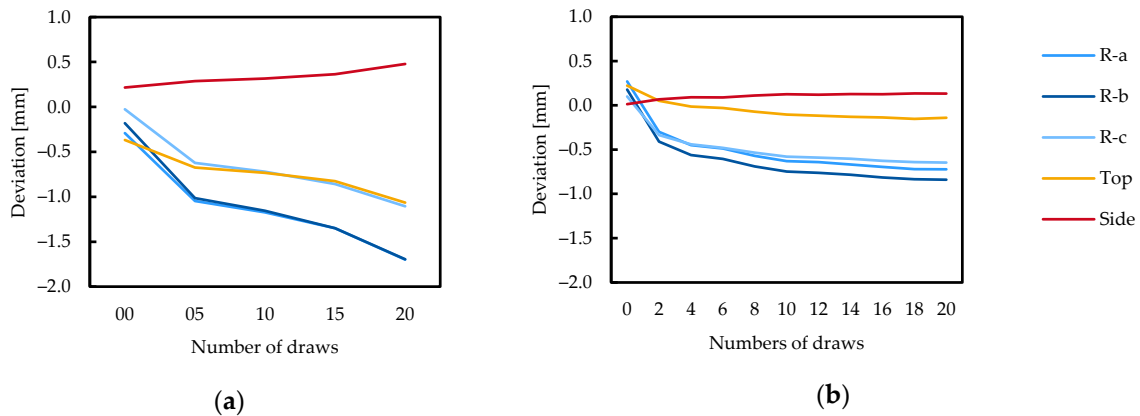

Figure 19. Course of deviation values of different measuring points of punch during 20 drawing operations compared to the CAD reference geometry: (**a**) deviation values of PLA_001 punch; (**b**) deviation values of PLA_002 punch.

4. Discussion

The printed polymer tools followed predicted behavior in terms of initial deformations based on tensile and flexural strengths of the materials. CF-reinforced PA, as a high-performance material with higher tensile strength, resisted deformation much better than PLA. The hypothesis that materials having high tensile strengths tend to have high compressive strength was confirmed for CF-PA and PLA, since the CF-PA tools compressed less than PLA tools. In addition, the increases in deformations of printed tools were higher for PLA compared to those of CF-reinforced PA, confirming the proposed hypothesis. Maximum deviations were experienced on the punch nose radius (R-a, R-b, and R-c), with deviations growing faster on both materials at these points compared to other pre-defined points (cf. Figure 12b). The second-highest growth in tool deformation was observed on the punch top. These deformation behaviors also confirm that the compressive strength at the punch nose radius is the limiting factor of these polymer materials for this application. The deformation of the die (R-d, R-e, R-f, and side) exhibited a minimal increase, indicating lesser forces experienced by these points, and hence not critical parameters in this particular example. An interesting change in deformation behavior was observed in PLA's first trial after 15 drawing operations (cf. Figure 19a). The increase in deformation growth indicates that after a certain amount of deformation (percent deformation), the material deforms more. This behavior was not observed in PLA's first trial and CF-PA, indicating that these materials did not cross the threshold deformation (percent deformation) during the 20 drawing operations to exhibit that behavior. The damage mechanism behind this threshold deformation was not found.

The shrinkage behavior of PLA turned out to be reduced compared to CF-PA, with lesser deviations of printed tools compared to CAD model before any drawing operations. The incorporation of shrinkage and deformation allowances showed a positive effect on tool accuracy and precision in terms of deformations. Not only was the initial deviation behavior improved by adding allowances, but also the increase of these deformations was flattened. One possible explanation for this behavior is that lower deviations before any drawing operations will result in a favorable load state compared to a more deformed tool. As the tool deforms, the forces applied to the tools might increase, making the next deformation even higher. Similar behavior was observed in the clearance between punch and die. More accurate clearance between the punch and die (smaller clearance after adding allowances) lowered the forces on punch nose radius and flattened the deformation growth.
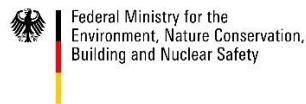
5. Conclusions

PLA is one of the cheapest and most easily available FFF materials on the market. Printing PLA is easier than CF-reinforced PA, and the printed parts have very good flat surfaces and finishes. Shrinkage is also minimal compared to CF-reinforced PA. The achieved dimensional accuracy of the first cup drawn with the PLA's first trial tool stayed within -1.02 to 0.96 mm. The resilience of PLA is less than that of CF-reinforced PA and the change of deviation came out to be -1.17 mm for 20 drawing operations (at the nose radius R-a). The cost of CF-reinforced PA used for the experiments is more than three times higher than that of PLA. Printing CF-reinforced PA is more difficult, and the printed parts have good flat surfaces but a rough surface finish. Shrinkage is more than for PLA but still predictable. Adding allowances to CF-PA similar to PLA's second trial could further improve the dimensional precision and accuracy of the cups. The achieved dimensional accuracy of the first cup drawn from CF-PA tool was in the range of -0.92 to 0.77 mm. The resilience of CF-reinforced PA is better than that of PLA, and the change in deviation turned out to be 0.05 mm on the flange radius R-d and 0.12 mm on the nose radius R-a for 20 drawing operations.

The dimensional accuracy of the drawn cups can be improved by introducing shrinkage and springback allowances. The properties of material related to these parameters and the geometrical shape of the part to be printed define the amounts of allowances. For thin features, such as the blank holder, no allowances are needed. After introducing allowances, the dimensional accuracy for PLA first drawn cup improved from a deviation range of -1.02 to 0.96 mm, to -0.71 to 0.33 mm. In addition, the durability of PLA improved in terms of change in deviation throughout the 20 drawing operations.

The application of PLA and CF-PA for deep drawing still poses challenges to achieving higher accuracy and repeatability, but this study provides a basis to further tweak some parameters to achieve those goals. As a prospect, a detailed study of shrinkage behavior and the deformation plus springback allowances for different sizes of the standard cup shapes could be performed to bridge the gap between the drawn part and the CAD model. Another interesting study would be to print the polymer tools at a higher infill percentage (reaching up to 100%) and observe its effect on deformation behavior and its growth in the printed tools. CF-reinforced PA is more resistant to deformation increase. Hence, a study to compare different reinforcement materials in polymers for deep drawing could add value to this research area of direct polymer additive tooling.

Author Contributions: Conceptualization, B.L. and A.S.; methodology, B.L.; software, A.S.; validation, B.L. and A.S.; formal analysis, B.L. and A.S.; investigation, A.S.; resources, G.B.; data curation, B.L. and A.S.; writing—original draft preparation, B.L. and A.S.; writing—review and editing, G.B. and F.F.; visualization, B.L. and A.S.; supervision, G.B.; project administration, G.B.; funding acquisition, B.L. and G.B. All authors have read and agreed to the published version of the manuscript.

Federal Ministry for the
Environment, Nature Conservation,
Building and Nuclear Safety

Appendix A

Table A1. List of material abbreviations and chemical formulae.

Abbreviation	Meaning	Chemical Formula
PLA	Polylactic acid	$C_3H_4O_2$
PC	Polycarbonate	$C_{16}H_{16}O_4$
CPE	Chlorinated polyethylene	C_4H_7Cl
ABS	Acrylonitrile butadiene styrene	$C_8H_8 \cdot C_4H_6 \cdot C_3H_3N$
PA6/66	Polyamide (Nylon 66)	$C_{12}H_{22}N_2O_2$
PA12	Polyamide (Nylon 12)	$C_{12}H_{23}NO$
PA-CF	Polyamide (Nylon 6) + carbon fiber	$C_6H_{11}NO + CF$
PA12-CF	Polyamide (Nylon 12) + carbon fiber	$C_{12}H_{23}NO + CF$
PEEK	Polyether ether ketone	$C_{19}H_{12}O_3$
PEEK-CF	Polyether ether ketone + carbon fiber	$C_{19}H_{12}O_3 + CF$

References

1. Kolbe, J. Thermisch Beschichtete, Faserverstärkte Polymerwerkzeuge für die Umformung Höherfester Blechwerkstoffe. Ph.D. Thesis, Technischen Universität Dortmund, Dortmund, Germany, 13 August 2012.
2. Deiler, G. Untersuchungen zum Eignungsprofil Polymerer Werkzeugwerkstoffe für das Tiefziehen von Feinblechen. Ph.D. Thesis, Universität Hannover, Hannover, Germany, 27 June 2005.
3. Frank, C. Kunststoff als Werkzeugwerkstoff für das Tiefziehen von Feinblechen. Ph.D. Thesis, Universität Hannover, Hannover, Germany, 24 November 1999.
4. Kampker, A.; Triebs, J.; Kawollek, S.; Ayvaz, P.; Beyer, T. Direct polymer additive tooling—Effect of additive manufactured polymer tools on part material properties for injection moulding. *RPJ* **2019**, *25*, 1575–1584.
5. Kampker, A.; Ayvaz, P.; Lukas, G. Direct Polymer Additive Tooling—Economic Analysis of Additive Manufacturing Technologies for Fabrication of Polymer Tools for Injection Molding. *KEM* **2020**, *843*, 9–18. [CrossRef]
6. Schuh, G.; Bergweiler, G.; Lukas, G.; Oly, M. Towards Temperature Control Measures for Polymer Additive Injection Molds. *Procedia CIRP* **2020**, *93*, 90–95. [CrossRef]
7. Danby, M.R.; Reznar, J.F. Metal-Stamping Die Manufactured by Additive Manufacturing. U.S. Patent 201313795495 20130312, 12 March 2013.
8. Müller, B.; Hund, R.; Malek, R.; Gerth, N. Laser Beam Melting for Tooling Applications—New Perspectives for Resource-Efficient Metal Forming and Die Casting Processes. In *Digital Product and Process Development Systems*; Kovács, G.L., Kochan, D., Eds.; Springer: Berlin/Heidelberg, Germany, 2013; pp. 124–137.
9. Durgun, I. Sheet metal forming using FDM rapid prototype tool. *RPJ* **2015**, *21*, 412–422. [CrossRef]
10. Aksenov, L.B.; Kononov, I.Y. 3D Printed Plastic Tool for Al Thin-Sheet Forming. *IOP Conf. Ser. Earth Environ. Sci.* **2019**, *337*, 12053. [CrossRef]
11. Nakamura, N.; Mori, K.-I.; Abe, Y. Applicability of plastic tools additively manufactured by fused deposition modelling for sheet metal forming. *Int. J. Adv. Manuf. Technol.* **2020**, *108*, 975–985. [CrossRef]
12. Schuh, G.; Bergweiler, G.; Bickendorf, P.; Fiedler, F.; Colag, C. Sheet Metal Forming Using Additively Manufactured Polymer Tools. *Procedia CIRP* **2020**, *93*, 20–25. [CrossRef]
13. Cheah, C.M.; Chua, C.K.; Lee, C.W.; Lim, S.T.; Eu, K.H.; Lin, L.T. Rapid Sheet Metal Manufacturing. Part 2: Direct Rapid Tooling. *Int. J. Adv. Manuf. Technol.* **2002**, *19*, 510–515. [CrossRef]

14. Du Hui, Z.; Kai, C.C.; Sen, C.Y.; Gek, L.-L.K.; Tiak, L.S. Advanced Sheet Metal Manufacturing using Rapid Tooling. In Proceedings of the 2000 International Solid Freeform Fabrication Symposium, Austin, TX, USA, 7–9 August 2000.

15. Leacock, A.; Volk, G.; McCracken, D.; Brown, D. The use of Fused Deposition Modelled Tooling in Low Volume Production of Stretch Formed Double Curvature Components. *Procedia Eng.* **2017**, *183*, 343–350. [CrossRef]

16. VDI 3405. *Additive Manufacturing Processes, Rapid Manufacturing. Figure 5*; Beuth Verlag GmbH: Berlin, Germany, 2019.

17. Fiberthree F3 PA-CF Pro Filament. Available online: https://www.3dmensionals.de/fiberthree-f3-pa-cf-pro-filament?number=PSUFT0005V (accessed on 7 July 2020).

18. Ultimaker PLA Filament. Available online: https://www.igo3d.com/ultimaker-3-pla (accessed on 7 July 2020).

19. Ultimaker CPE Filament. Available online: https://www.igo3d.com/ultimaker-3-cpe (accessed on 7 July 2020).

20. PEEK Filament von Intamsys. Available online: https://www.3dmensionals.de/peek-filament-von-intamsys (accessed on 7 July 2020).

21. Fiberlogy PA12 + CF Karbonfaserversärkt. Available online: https://shop.bfi-it.de/fiberlogy-pa12-cf-karbonfaserversaerkt-1.75mm-0.5kg (accessed on 7 July 2020).

22. Polyamid PA6/66. Available online: https://shop.bigrep.com/product/polyamid-pa6-66/ (accessed on 7 July 2020).

23. Polymaker PolyMide™ PA6-CF Filament. Available online: https://www.3dmensionals.de/polymaker-polymide-pa6-cf-filament (accessed on 7 July 2020).

24. Ultimaker ABS Filament. Available online: https://www.igo3d.com/ultimaker-3-abs (accessed on 7 July 2020).

25. Ultimaker PC Filament. Available online: https://www.igo3d.com/ultimaker-3-pc-filament (accessed on 7 July 2020).

26. 3DXTech CarbonX—Carbon-PEEK Filament. Available online: https://www.filamentworld.de/shop/high-performance-filament/peek-filament/3dxtech-carbonx-1-75-mm-carbon-peek/ (accessed on 29 November 2020).

27. DIN EN 10130. *Cold Rolled Low Carbon Steel Flat Products for Cold Forming*; Beuth Verlag GmbH: Berlin, Germany, 2007.

28. Limiting Drawing Ratio (LDR) Test/Swift Deep Drawing Cup Test. Available online: https://www.zwickroell.com/en/materials-testing/sheet-metal-testing/earing-test/limiting-drawing-ratio-test-ldr (accessed on 29 November 2020).

29. Dietrich, J. Tiefziehen. In *Praxis der Umformtechnik*, 12th ed.; Springer Fachmedien Wiesbaden: Wiesbaden, Germany, 2018; p. 178.

30. Fritz, A.H. Umformen. In *Fertigungstechnik*, 12th ed.; Springer: Berlin/Heidelberg, Germany, 2018; p. 178.

31. How to Print with Ultimaker PLA. Available online: https://support.ultimaker.com/hc/en-us/articles/360011952740-How-to-print-with-Ultimaker-PLA (accessed on 29 November 2020).